https://doi.org/10.1051/e3sconf/202457201004

Dynamic simulation of different vertical axis micro wind turbines serving a typical house in Italy: assessment of energy, environmental and economic impacts

Antonio Rosato[1], *Achille* Perrotta[1,*], *Luigi* Maffei[1]

[1] Built Environment Control Laboratory RIAS, Department of Architecture and Industrial Design, University of Campania Luigi Vanvitelli, 81031 via San Lorenzo 4 (Aversa), Italy

Abstract. Scientific interest on small-scale wind turbines (power output lower than 50 kW) is significantly increased in the last years. In this paper the performance of four commercial models of small-scale vertical axis wind turbines (with different power outputs of 1100, 2200, 3100 and 6300 W) serving a typical single-family house have been analyzed by means of the TRaNsient SYStems simulation tool (TRNSYS) upon varying the climatic conditions of 5 Italian cities (Naples, Rome, Milan, Palermo, Alghero). Their performance has been compared with those corresponding to the same building while served by the central electric grid from energy, environmental and economic points of view. The simulations highlighted that the utilization of wind turbine allows to reduce the electric energy imported from the grid, the equivalent global CO_2 emissions and the operating costs up to 59.36%, 59.68% and 142.39%, respectively. The study revealed that both the commercial model of the wind turbine model as well as the installation city greatly affect the performance. Specifically, the best results have been achieved for the 2200 W wind turbine, whatever the city is; for a given wind turbine model, the minimum simple pay-back period (1.3 years) is obtained for the city of Palermo.

1 Introduction

1.1 Background

The increasing number of people on the planet has led to a rise in the use of fossil fuels and the resulting emissions of greenhouse gases, with residential buildings being responsible for the majority of the energy used worldwide (as underlined by the International Energy Agency [1]). According to the new Energy Performance of Buildings Directive, Member States must ensure that the average energy consumption of residential building stock decreases by at least 16% by 2030. It is well known that promoting the use of renewable energy sources is one of the most promising ways to reduce primary energy demand and mitigate climate change [1,2]. Many nations have embraced technologies based on renewable sources to generate clean and limitless energy to meet their ever-increasing demands.

Wind power is among the most widely used renewable sources [2]. The utilization of wind turbines to transform wind energy into electrical power is one of the renewable energy source-based options that is quickly gaining popularity and has drawn a lot of interest from the scientific community over the last decades [2-5]. The rated output power may be used to classify them [6,7] as follows: (i) large-scale, (ii) medium-scale, and (iii) small-scale wind turbines.

Small-scale wind turbines (SWTs) are defined as having an electric output of up to 50 kW by the International Commission of Electrotechnics [8]. They are installed on the "customer" side of the electric meter or close to the location where the energy they produce will be used. Usually, they are employed in small-scale commercial, industrial, residential, and agricultural settings. They are either directly linked to the central grid to assist grid operations or balance off huge loads nearby, or they are used to meet the on-site load. They may also be utilized in hybrid energy systems that combine batteries, micro-cogeneration units, photovoltaics, and other distributed energy sources. SWTs have many benefits over large- and medium-scale wind energy systems, including lower maintenance costs, increased dependability, a wider wind speed operation range, the ability to start on their own at lower wind speeds, less installation space requirements, a decreased reliance on grid-connected power and lengthy transmission lines, lower capital costs, etc. SWTs are a more adaptable option for homeowners who might not have a lot of land or a sunny south-facing roof for solar panels because they can also be installed at low altitudes in a variety of locations, including rooftops and even in some urban settings [3,7,9]. As a result, SWTs have the potential to be used and integrated into residential urban environments. Despite these benefits, designing and operating building integrated-SWTs is not without its

* Corresponding author: achille.perrotta@unicampania.it

difficulties. First of all, it should be taken into account that the potential of wind turbines depends on factors like wind speed and installation site; therefore, creating a consistent and dependable energy source can be difficult in metropolitan settings due to the fluctuating behaviour of wind [3,7,9,10]. Furthermore, a SWT operating in real life is exposed to wind that changes direction and speed suddenly; manufacturers' power curves do not account for this transition period, during which the power output will decrease significantly as a result of the SWT attempting to adjust to the new conditions. This could have a substantial impact on the design phase's evaluation of the SWT's performance [3,7,9-11]. Lastly, a significant barrier to the efficient installation of SWTs in urban settings is the absence of reliable methods for calculating the energy yield and wind speed at possible turbine mounting locations [3,7,9-11].

There are basically two types of SWTs [12,13]: (i) horizontal axis small-scale turbines (HASWTs); (ii) vertical axis small-scale wind turbines (VASWTs). HASWT have horizontal axis of rotation, i.e., parallel to the wind stream, whereas VASWTs are characterized by a vertical axis of rotation, i.e., perpendicular to the wind stream. While VASWTs may use wind from any direction (i.e., they are omnidirectional in their functioning), HASWTs depend on the direction of the wind to function. Based on the type of rotor they use, VASWTs may be classified into two groups: the lift-based Darrieus type and the drag-based Savonius type. A hybrid Savonius-Darrieus design can be also found in certain models.

According to IEC 61400-2 [14], SWTs are generally categorized into the three different groups reported in Table 1 depending on the rated power output P_{rated} as well as the rotor swept area A: pico wind turbines (PWTs), micro wind turbines (MCWTs) and mini wind turbines (MNWTs).

Table 1. SWTs classification.

Category	Rated power P_{rated} (kW)	Rotor swept area A (m^2)
Pico wind turbines (PWTs)	$P_{rated} \leq 1$	$A \leq 4.9$
Micro wind turbines (MCWTs)	$1 \leq P_{rated} \leq 7$	$A \leq 40$
Mini wind turbines (MNWTs)	$7 \leq P_{rated} \leq 50$	$A \leq 200$

1.2 Methods, objectives and structure of the study

In this work, the performance of 4 commercial vertical axis micro wind turbines (VAMCWTs) have been studied via the dynamic TRaNsient SYStems simulation tool (TRNSYS) [15] (version 16) in the case of a typical single-family house is served while located into 5 different cities in Italy (Naples, Rome, Milan, Palermo and Alghero); the performance of the building-integrated VAMCWTs have been compared with that one of a reference scenario where the same single-family house is served by the central grid only in order to assess the potential savings in terms of imported electric energy, equivalent global CO_2 emissions, operating costs.

The main goals of the paper can be summarized as reported below:

- assess the potential energy, economic, and environmental benefits associated with the use of VAMCWTs compared to a traditional scenario in the case of a typical residential utility in the Italian context,
- evaluate the effects of installation Italian cities (and, therefore, boundary climatic conditions) on the performance of building-integrated VAMCWTs;
- support the diffusion and use of energy systems based on the harnessing of renewable wind energy through VAMCWTs.

Section 2 describes the building electric load, the selected wind turbines, as well as the adopted simulation model and corresponding climatic data; section 3 reports the simulations results, while section 4 discusses the results of the comparison between proposed SWT-integrated building and the reference scenario without SWTs upon varying the Italian city.

2 Building electric load, wind turbines, simulation model and climatic data

In this section the electric demand of a typical building assumed as reference (sub-section 2.1), the micro wind turbines (sub-section 2.2), the model adopted for simulating the selected wind turbines as well as the climatic data (sub-section 2.3) are described.

2.1 Building electric demand profile

It's well known that the electric consumption of residential buildings is affected by a significant number of parameters. For this reason, an innovative tool developed by the Loughborough University based on a stochastic approach [16] has been used to model the daily electric energy demand profiles associated to the operation of domestic appliances and lighting systems. The tool allows to determine these profiles according to the maximum number of persons, the type of day (weekday or weekend), the month of the year, the number and types of domestic appliances (without a detailed definition of the building); then, the number of persons as well as the activation of both domestic appliances and lighting systems are randomly defined by the tool and the related electric consumption is calculated. This tool doesn't take into account the electric demand associated to cooking devices, water heating as well as air-conditioning systems. In this study, a maximum of 4 persons is assumed. The following domestic appliances are considered taking into account that they are the most used ones with reference to Italian residential houses: 1 fridge-freezer, 1 fridge, 1 clock, 1 phone, 1 iron, 1 vacuum, 1 personal computer, 1 printer, 2 TVs, 1 microwave, 1 dish washer, 1 washing machine. The annual electric demand profile of the building assumed as reference has been obtained by combining 365 different daily electric demand profiles characterized by a time-step of 1 minute. Figure 1 reports the annual electric demand profile as a function of the time. According to this figure, the electric demand presents a maximum of 4383 W (due to the simultaneous operation of most of the selected electric appliances and lighting systems during September 8th, according to the random allocation performed by the stochastic tool used in this study) and a minimum of 21 W.

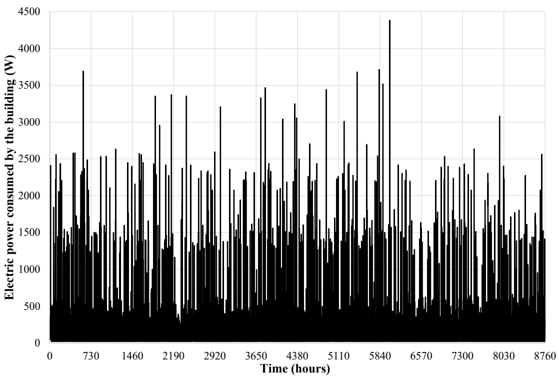

Fig. 1. Annual electric demand profile of the building as a function of the time.

Figure 2 shows the electric load-duration diagram (corresponding to the utilization of lighting and domestic appliances) with the values sorted in descending order. This plot indicates that the duration of the electric demand covers the entire year. According to Figs. 1 and 2, the annual electric consumption of the reference building is 2408.96 kWh.

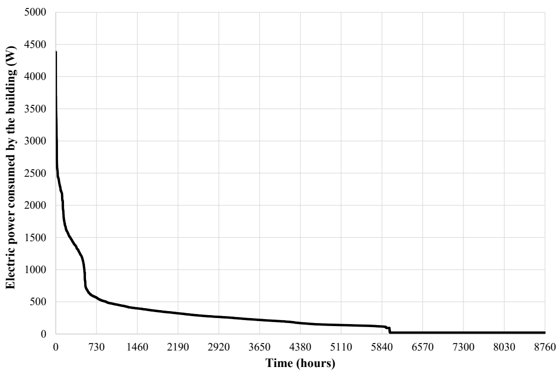

Fig. 2. Annual electric load-duration diagram of the building.

2.2 Selected wind turbines

Four different VAMCWTs commercially available in Italy have been analyzed in this study. Table 2 reports the type (Savonius or Darrieus or hybrid), manufacturer, model, number of blades, start-up wind speed (the minimum wind speed required for the blades and the rotor to starts spinning, without providing any usable electric power), cut-in wind speed (which is the speed at which a wind turbine begins producing energy), cut-out wind speed (which is the highest wind speed at which a wind turbine is intended to produce useable power), and maximum power output, rotor diameter, turbine length, tower height, capital cost and specific capital costs of the selected wind turbines. In more detail, the maximum power output of the selected VAMCWTs ranges from 1100 W up to 6300 W.

2.3 Simulation model and climatic data

The TRaNsient SYStems simulation tool (TRNSYS) [15] (version 16) has been used in this study to model the wind turbine operation and the climatic conditions.

Table 2. Selected vertical axis micro wind turbines.

Type/ Company/ Model/ Blades' number	Start-up/ Cut-in/ Cut-off wind speed (m/s)	Max. power (W)	Rotor diameter/ Turbine length/ tower height (m)	Capital cost (€)/ Specific capital cost (€/W)
Savonius/ FLTXNY/ FS-1000/ 2 [17]	1.5/ 2.0/ 14.0	1100	0.67/ 1.5/ 7.0÷12.0	562.31/ 0.51
Savonius/ FLTXNY/ FS-2000/ 2 [17]	1.5/ 2.0/ 14.0	2200	0.8/ 2.0/ 7.0÷12.0	684.39/ 0.33
Hybrid Savonius-Darrieus/ Etneo/ DS3000/ 3 [18,19]	2.0/ 2.8/ 14.0	~3100	4.0/ 4.16/ 4.0	17500.00 / 5.65
Darrieus/ AEOLOS/ Aeolos-V/ 3 [20-22]	1.5/ 1.5/ 14.0	~6300	4.5/ 4.8/ 4.8	13746.98 / 2.29

Because it considers the transient nature of occupant-driven loads, the part-load features of generating systems, and the interactions between building loads, system outputs, and climatic data, this tool is frequently utilized in the scientific field for detailed modelling of energy systems [23-25].

Each component of a thermodynamic system is represented in TRNSYS by a FORTRAN source code model called "Type". In this case, the TRNSYS Type 90 has been used to model the performance of the selected VAMCWTs. This model requires the definition of 6 parameters (Table 3) and 6 inputs (Table 4) to obtain 3 outputs (Table 5).

The turbine power loss has been assumed equal to 0, while a site shear exponent of 0.26 has been considered in order to model obstructed airflow. The TRNSYS Type 90 models the performance of the wind turbine mainly based on its performance curve representing the power output as a function of the wind velocity (input 6).

Table 3. Parameters of the TRNSYS Type 90.

 https://doi.org/10.1051/e3sconf/202457201004

1	Site elevation (m)
2	Data collection height (m)
3	Hub height (m)
4	Turbine power loss
5	Number of turbines
6	Logical unit of the containing power data

Table 4. Inputs of the TRNSYS Type 90.

1	Control signal
2	Wind velocity (m/s)
3	Ambient temperature (°C)
4	Site shear exponent
5	Barometric pressure (atm)
6	External file with the performance curve of the wind turbine (-)

Table 5. Outputs of the TRNSYS Type 90.

1	Power output (W)
2	Turbine hours (h)
3	Power coefficient (-)

Figure 3 shows the performance curves of the selected VAMCWTs suggested by the manufacturers and provided as input 6 to the TRNSYS Type 90 in this study; these curves indicate the ranges of both power output and wind speed (from the start-up up to the cut-out) corresponding to each wind turbine; the values refer to an height above the ground of 9 m, 9 m, 8 m and 4.8 m in the cases of the turbines FS-1000, FS-2000, DS-3000 and Aeolos-V, respectively.

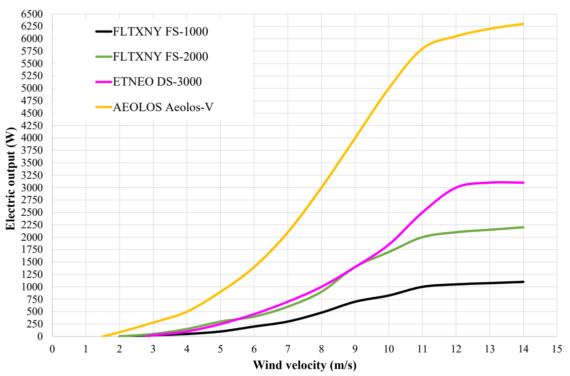

Fig. 3. Performance curves of the selected VAMCWTs based on manufacturer data.

The weather conditions (wind velocity, outside temperature and atmospheric pressure) required by the TRNSYS Type 90 as inputs 2, 3 and 5 have been defined (together with the site elevation) according to the Typical Meteorological Year version 2 weather database (TMY2) [26] by means of the TRNSYS Type 15-6 that is a weather data processor providing one year's worth of data available to other TRNSYS components by reading it from an external weather data file at regular intervals. Effective estimation of wind turbine performance is made possible by this Type, which allows to consider climate variables that are actually reflective of the city. In this study, 5 different cities in Italy (Naples, Rome, Milan, Palermo and Alghero) have been considered in order to take into account different Italian climatic conditions. These cities are reported in Figure 4 and they are characterized by the following coordinates:
- Naples: latitude 40° 51' 11.8584" North, longitude 14° 18' 20.0628' East;
- Rome: latitude 41° 54' 10.0152" North, longitude 12° 29' 46.9176" East;
- Milan: latitude 45° 27' 51.1596" North, longitude 9° 11' 28.9788" East;
- Palermo: latitude 38° 7' 0.0084" North, longitude 13° 22' 0.0012" East;
- Alghero: latitude 40° 33' 55.48" North, longitude 8° 19' 15.31" East.

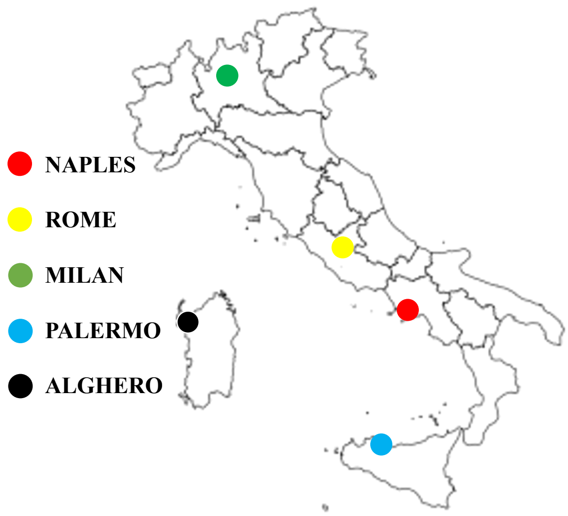

Fig. 4. Cities of Italy where the selected VAMCWTs are installed.

Figure 5 describes the annual wind velocity-duration diagrams as a function of the Italian cities selected in this study, with the values sorted in descending order. This figure shows that Palermo is characterized by the maximum annual average wind velocity, while the minimum annual average wind speed is associated to the city of Milan. In particular, the mean annual wind speed is 2.48 m/s, 3.19 m/s, 1.10 m/s, 4.24 m/s, and 3.19 m/s in the cases of Naples, Rome, Milan, Palermo and Alghero, respectively.

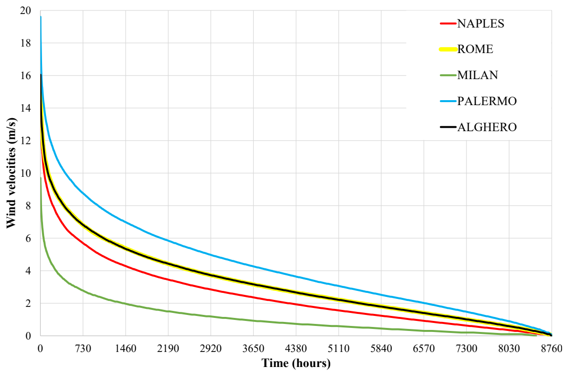

Fig. 5. Annual wind velocity-duration diagrams as a function of the Italian city.

3 Simulation results

The simulations have been performed with reference to an entire year (by setting a simulation time-step of 1 minute). In this section the simulation results are reported and described. Figures 6a and 6b show two examples of daily operation of the proposed configuration including one of the selected wind turbines; in particular, Figures 6a and 6b report the building power demand, power generated by the wind turbine, power generated by the wind turbine and sold to the grid, power purchased from the grid to cover the electric demand as well as wind speed as a function of the time, in the case of the model FS-2000 is used in Naples on April 15th and September 8th (day characterized by the maximum electric demand), respectively.

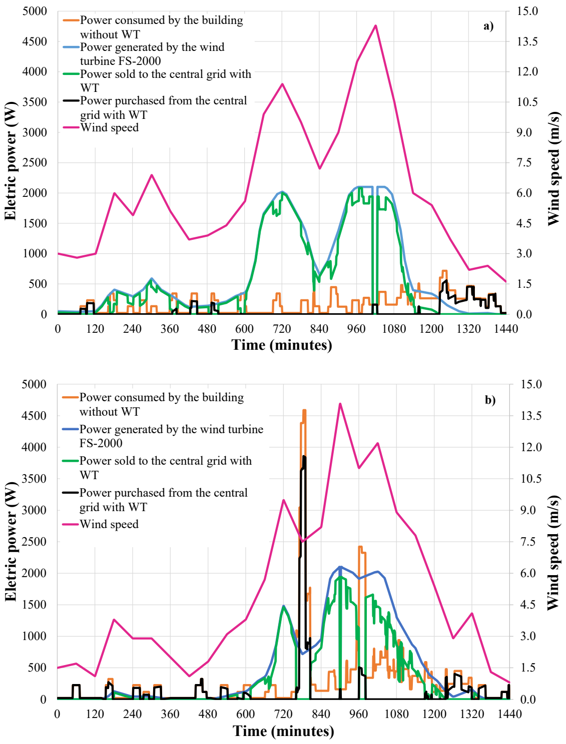

Fig. 6. Example of typical daily operation of the wind turbine model FS-2000 in Naples on April 15th (a) and September 8th (b).

Figure 7 reports the annual electric energy generated by the selected 4 VAMCWTs as a function of both the wind turbine model and the city.

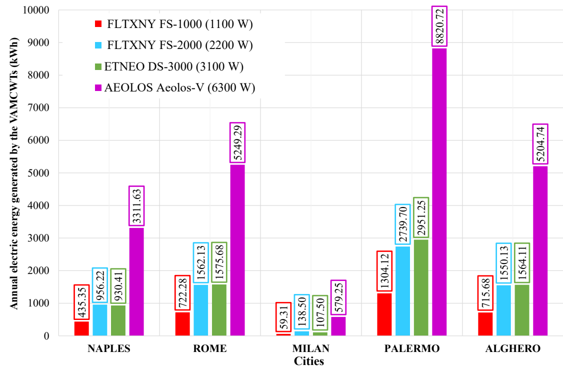

Fig. 7. Annual electric energy generated by the VAMCWTs.

This plot indicates that, for a given city, the greater the capacity of the wind turbine, the greater the electric energy generation; as a consequence, the maximum value correspond to the wind turbine Aeolos-V, while the minimum corresponds the wind turbine FS-1000. In addition, it can be underlined that, whatever the wind turbine model is, the generated annual electric energy is maximum in the case of the city of Palermo (characterized by the highest annual average wind speed, as indicated in Figure 5), while it is minimum in Milan (characterized by the lowest annual average wind speed, as indicated in Figure 5). In particular, the values vary between a minimum of 59.31 kWh up to a maximum of 8820.72 kWh.

In the case of the electric power generated by the wind turbine is larger than the building electric demand, the surplus is sold to the electric central grid. Figure 8 reports the annual electric energy sold to the electric central grid as a function of both the wind turbine model and the city.

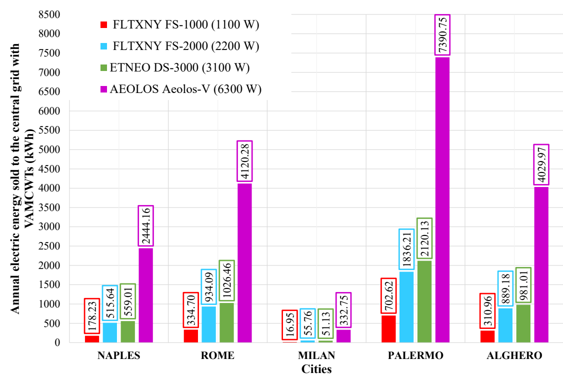

Fig. 8. Annual electric energy sold to the central grid.

The plot indicates that, for a given city, the greater the capacity of the wind turbine, the greater the electric energy sold to the electric central grid. In addition, it can be derived that, for a given wind turbine model, the wind velocity significantly affects the results. In particular, the values indicated in this figure range from a minimum of 16.95 kWh in the case of the wind turbine FS-1000 (characterized by the lowest nominal electric output) operating in Milan (characterized by the lowest annual average wind speed) up to a maximum of 7390.75 kWh in the case of the wind turbine Aeolos-V (characterized by the highest nominal electric output) operating in Palermo (characterized by the highest annual average wind speed).

In the case of the electric power generated by the wind turbine is lower than the building electric demand, the difference has to be purchased from the electric central grid. Figure 9 reports the annual electric energy purchased from the central grid as a function of both the wind turbine model and the city.

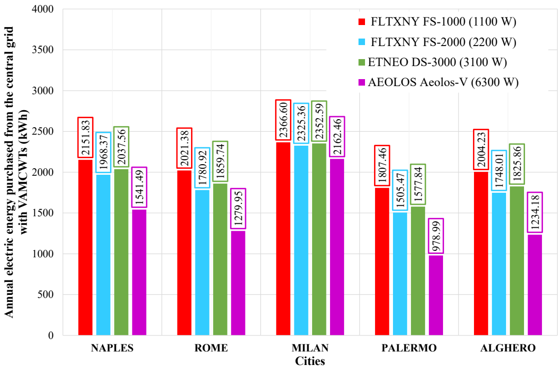

Fig. 9. Annual electric energy purchased from the grid.

This graph indicates that, for a given city, the greater the capacity of the wind turbine, the lower the annual electric energy purchased from the grid. In addition, it can be noticed that, for a given model of wind turbine, the annual electric energy purchased from the grid is minimum for the city of Palermo (characterized by the highest annual average wind speed), while it is maximum in the case of Milan (characterized by the lowest annual average wind speed). For a given city, the annual electric energy purchased from the grid is minimum for the wind turbine Aeolos-V (characterized by the highest nominal electric output), while it is maximum in the case of the wind turbine FS-1000 (characterized by the lowest nominal electric output). In greater detail, the minimum value in this figure is 978.99 kWh, while the maximum value is equal to 2366.60 kWh.

4 Comparison of the proposed systems with the reference scenario

In this study, the performance of the proposed scenario where the building is connected to both the central grid and the wind turbine have been contrasted against those corresponding to the reference scenario corresponding to the building connected to the central grid only, without the wind turbine. This comparison has been carried out in order to determine the potential savings in terms of primary energy consumption, equivalent global CO_2 emissions and operating costs; as a result, the appropriateness of the building-integrated wind turbine compared to the conventional scheme has been assessed.

4.1 Energy comparison

The percentage difference ΔE_{el} between the annual electric energy $E^{PS}_{el,imp}$ imported from the grid in the case of the proposed scenario (including the wind turbine) and the annual electric energy $E^{RS}_{el,imp}$ imported from the grid in the case of the reference scenario (without the wind turbine) has been calculated as follows:

$$\Delta E_{el} = \frac{E^{PS}_{el,imp} - E^{RS}_{el,imp}}{E^{RS}_{el,imp}} \quad (1)$$

Figure 10 reports the values of ΔE_{el} as a function of both the wind turbine model and the city. All the values reported in this figure are negative, meaning that the proposed scenario with the wind turbine allows to reduce the electricity imported from the grid with respect to the reference scenario, whatever the wind turbine model and the city are. In greater detail, this figure indicates that, for a given city, the utilization of the wind turbine allows to reduce the electric energy imported from the grid from a minimum of -1.76% in the case of the wind turbine FS-1000 (wind turbine characterized by the lowest nominal electric output) operating in Milan (city characterized by the lowest annual average wind speed) up to a maximum of -59.36% in the case of the wind turbine Aeolos-V (wind turbine characterized by the highest nominal electric output) operating in Palermo (city characterized by the highest annual average wind speed).

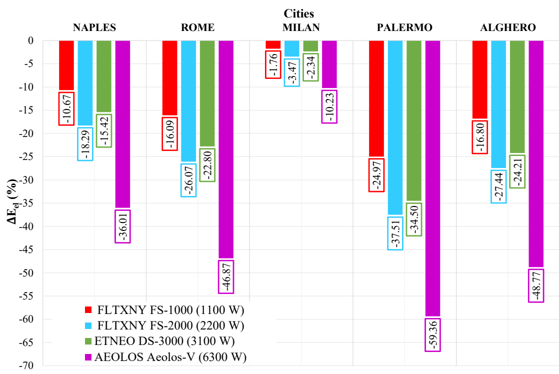

Fig. 10. ΔE_{el} as a function of the wind turbine model and city.

4.2 Environmental comparison

This study evaluated the environmental effects by using the Chicco and Mancarella [27] energy output-based emission factor method; it yields the global equivalent mass m_x of a given pollutant x emitted while producing the energy output E according to the following formula:

$$m_x = u^E_x \cdot E \quad (2)$$

where u^E_x is the specific emissions of x per unit of E (so-called "energy output-based emission factor"). It is dependent on a number of structural and operational parameters, including the equipment type, the operation at partial loads, the age, the maintenance status, the ambient conditions, and the systems for pollutant abatement. Although every kind of pollutant and system's emissions can be taken into account using Eq. (2), CO_2 emissions generally show to be quantitatively far more significant than emissions of other pollutants [28]. The CO_2 emission factor associated to the electricity generation in Italy $u_{CO_2}^{E_{el}}$ depends on the location, the day as well as the time of the day. Figure 11 reports this factor as a function of the time in the cases of the Italian cities selected in this study according to the values suggested in [28].

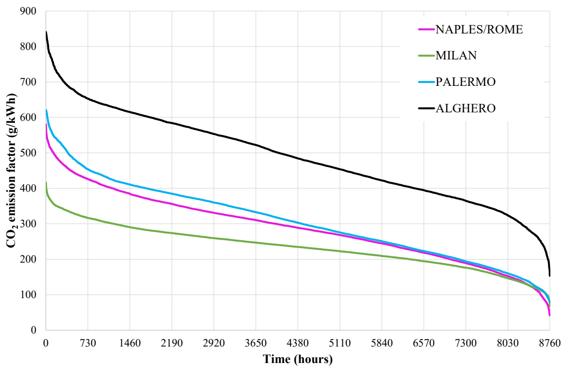

Fig. 11. CO_2 emissions factor as a function of city and time.

The percentage difference ΔCO_2 between the global equivalent CO_2 emissions CO_2^{PS} in the case of the proposed scenario (including the wind turbine) and the global equivalent CO_2 emissions CO_2^{RS} in the case of the reference scenario (without the wind turbine) has been obtained via the following formula:

$$\Delta CO_2 = \frac{CO_2^{PS} - CO_2^{RS}}{CO_2^{RS}} = \frac{\sum_i u_{CO_2,i}^{E_{el}} \cdot P_{el,imp,i}^{PS} \cdot STS - \sum_i u_{CO_2,i}^{E_{el}} \cdot P_{el,imp,i}^{RS} \cdot STS}{\sum_i u_{CO_2,i}^{E_{el}} \cdot P_{el,imp,i}^{RS} \cdot STS} \quad (3)$$

where $u_{CO_2,i}^{E_{el}}$ is the i-th CO_2 emission factor corresponding to the i-th electric power imported from the grid in the case of the proposed scenario ($P_{el,imp,i}^{PS}$) or in the case of the reference scenario ($P_{el,imp,i}^{RS}$) at the same simulation time, while STS is the simulation time step (assumed constant and equal to 1 minute).

Figure 12 reports the values of ΔCO_2 as a function of both the wind turbine model and the city of installation. All the values reported in this figure are negative; this means that the proposed scenario with the wind turbine allows to reduce the global equivalent CO_2 emissions in comparison to the reference scenario, whatever the wind turbine model or city is. In particular, this figure indicates that, for a given city, the utilization of the wind turbine allows to reduce the CO_2 emissions with respect to the reference scenario with a minimum of -1.75 % in the case of the wind turbine FS-1000 (wind turbine characterized by the lowest nominal electric output) operating in Milan (city characterized by the lowest annual average wind speed) up to a maximum of -59.68% in the case of the wind turbine Aeolos-V (wind turbine characterized by the highest nominal electric output) operating in Palermo (city characterized by the highest annual average wind speed).

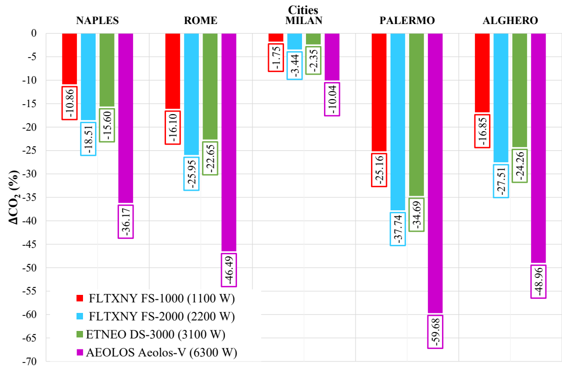

Fig. 12. ΔCO_2 as a function of the wind turbine model and city.

4.3 Economic comparison

The percentage difference ΔOC between the operating costs OC^{PS} (due to the electricity imported from the grid) reduced by the annual revenue $REV_{el,sold}$ obtained thanks to the electricity sold to the central grid $E_{el,sold}^{PS}$ in the case of the proposed scenario (including the wind turbine) and the operating costs OC^{RS} (due to the electricity imported from the grid) of the reference scenario (without the wind turbine) has been calculated via this formula:

$$\Delta OC = \frac{\left(OC^{PS} - REV_{el,sold}\right) - OC^{RS}}{OC^{RS}} = \frac{\left(UC_{el,imp} \cdot E_{el,imp}^{PS} - UC_{el,sold} \cdot E_{el,sold}^{PS}\right) - UC_{el,imp} \cdot E_{el,imp}^{RS}}{UC_{el,imp} \cdot E_{el,imp}^{RS}} \quad (4)$$

where $UC_{el,imp}$ and $UC_{el,sold}$ are, respectively, the unit cost of electricity purchased from the grid and the unit price of electric energy sold to the grid; the values of $UC_{el,imp}$ and $UC_{el,sold}$ have been assumed constant and equal to 0.26 €/kWh and 0.19 €/kWh, respectively, according to the current average Italian market scenario [29,30].

Figure 13 reports the values of ΔOC as a function of both the wind turbine model and the city. Whatever the wind turbine model or city is, all the values in this figure are negative; therefore, the proposed scenario with the wind turbine always allows to reduce the operating costs with respect to the reference scenario. In more detail, this plot underlines that, for a given city, the utilization of the wind turbine allows to reduce the operating costs in comparison to the reference scenario from a minimum of -2.27% in the case of the wind turbine FS-1000 (characterized by the lowest nominal electric output) operating in Milan (city characterized by the lowest annual average wind speed) up to a maximum of -142.39% in the case of the wind turbine Aeolos-V (characterized by the highest nominal electric output) operating in Palermo (city characterized by the highest annual average wind speed).

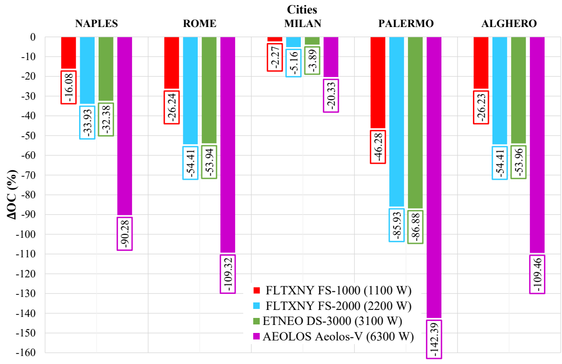

Fig. 13. ΔOC as a function of the wind turbine model and city.

With respect to the reference scenario, the utilization of the wind turbine allows to reduce the operating costs, but it requires an extra investment cost. The so-called simple payback period SPB represents the time required to recover the extra initial investment thanks to the operating costs savings and the revenues for electricity sold to the grid; it can be calculated as follows:

$$SPB = \frac{WT^{CC}}{(OC^{PS} - OC^{RS}) + REV_{el,sold}} = \frac{WT^{CC}}{(OC^{PS} - OC^{RS}) + E^{PS}_{el,sold} \cdot UC_{el,sold}} \quad (5)$$

where WT^{CC} is the capital cost of wind turbine. Figure 14 shows the values of SPB as a function of both the wind turbine model and the city. This plot shows that SPB ranges from a minimum of 1.3 years (in the case of the wind turbine FS-2000 operating in Palermo) up to a maximum of 718.1 years (in the case of the wind turbine DS-3000 operating in Milan). It indicates that all the turbines are suitable from an economic point of view (i.e., SPB is lower than the expected wind turbines' lifetime, that can be assumed equal to about 20÷25 years), except the turbine DS-3000 in Milan. The shortest SPB is obtained for the FS-2000 wind turbine, whatever the city is. This result is justified taking into account the reduced capital cost (684.39 €) of the FS-2000 wind turbine as well as its capability in reducing the electricity imported from the grid.

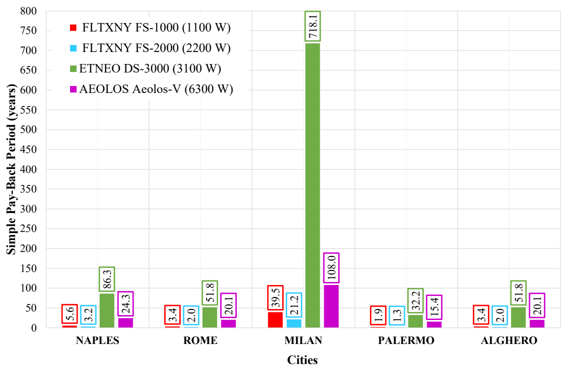

Fig. 14. SPB as a function of the wind turbine model and city.

5 Conclusions

In this study, the performance of four commercial models of small-scale vertical axis wind turbines (with different power output of 1100, 2200, 3100 and 6300 W) serving a typical single-family house have been assessed and compared with those corresponding to a reference scenario via the dynamic simulation TRNSYS upon varying the climatic conditions of 5 Italian cities (Napoli, Roma, Milano, Palermo, Alghero). The simulation outputs indicated that, whatever the wind turbine model and the city are, the utilization of the wind turbine allows to reduce the electric energy imported from the grid, the global CO_2 emissions and the operating costs up to about 59.36%, 59.68% and 142.39%, respectively. In particular, the best results have been obtained in the case of the wind turbine Aeolos-V (characterized by the highest nominal electric output of 6300 W) operating in Palermo (city characterized by the highest annual average wind speed), while the worst data have been achieved with reference to the wind turbine FS-1000 (characterized by the lowest nominal electric output) operating in Milan (city characterized by the lowest annual average wind speed). The shortest simple-pay back has been is obtained for the FS-2000 wind turbine, whatever the city is; it's 1.3 years in the case of Palermo. In the future, the authors would like to perform experimental tests in order to compare the simulation results with respect to the field performance.

References

1. 2021 Global Status Report for Buildings and Construction. Towards a Zero emission, Efficient and Resilient Buildings and Construction Sector. Available online: https://globalabc.org/sites/default/files/2021-10/GABC_Buildings-GSR-2021_BOOK.pdf (Accessed on 18 April 2024).
2. W.-T. Chong, W.K. Muzammil, K.-H. Wong, C.-T. Wang, M. Gwani, Y.-J. Chu, S.-C. Poh. Cross axis wind turbine: Pushing the limit of wind turbine technology with complementary design, Appl. Energy **207**, (2017): 78–97.
3. A.-S. Yang, Y.-M. Su, C.-Y. Wen, Y.-H. Juan, W.-S. Wang, C.-H. Cheng. Estimation of wind power generation in dense urban area, Appl. Energy **171**, (2016): 213–230.
4. X. Tang, X. Huang, R. Peng, X. Liu. A Direct Approach of Design Optimization for Small Horizontal Axis Wind Turbine Blades, Procedia CIRP **36**, (2015): 12-16.
5. P. Ying, Y.K. Chen, Y.G. Xu, Y. Tian. Computational and experimental investigations of an omni-flow wind Turbine, Appl. Energy **146**, (2015): 74-83.
6. R. Byrne, N.J. Hewitt, P. Griffiths, P. MacArtain. Observed site obstacle impacts on the energy performance of a large-scale urban wind turbine using an electrical energy rose, Energy Sustain. Dev. **43**, (2018): 23-37.

7. S.M. Weekes, A.S. Tomlin, S.B. Vosper, A.K. Skea, M.L. Gallani, J.J. Standen. Long-term wind resource assessment for small and medium-scale turbines using operational forecast data and measure–correlate–predict, Renew. Energy **81**, (2018): 760-769.
8. European Wind Energy Association. Wind Energy - The Facts: A guide to the technology, economics and future of wind power, Earthscan, United Kingdom, (2009): 1–592.
9. M.B. Kalashani, M. Seyedmahmoudian, S. Mekhilef, A. Stojcevski, B. Horan. Small-scale wind turbine control in high-speed wind conditions: A review, Sustain. Energy Technol. Assessments **60**, (2023).
10. K. Calautit, C. Johnstone. State-of-the-art review of micro to small-scale wind energy harvesting technologies for building integration, Energy Convers. Manag. **20**, (2023).
11. K.C. Anup, J. Whale, T. Urmee. Urban wind conditions and small wind turbines in the built environment: A review, Renew. Energy **131**, (2019): 268-283.
12. L.M. Kamp, L.F.I. Vanheule. Review of the small wind turbine sector in Kenya: Status and bottlenecks for growth, Renew. Sustain. Energy Rev. **49**, (2015): 470-480.
13. A. Tummala, R.K. Velamati, D.K. Sinha, V. Indraja, Krishna, V.H. A review on small scale wind turbines, Renew. Sustain. Energy Rev. **56**, (2016): 1351-1371.
14. International Standard IEC 61400-2:2013 - Wind turbines - Part 2: Small wind turbines, 3rd ed.; International Electrotechnical Commission: Geneva, Switzerland, 2013.
15. S.A. Klein, TRNSYS 16: A Transient System Simulation Program - Volume 1 Getting Started, Solar Energy Laboratory, University of Wisconsin, Madison, USA, 2007. Available online: https://web.mit.edu/parmstr/Public/Documentation/01-GettingStarted.pdf (Accessed on 18 April 2024).
16. E. McKenna, M. Thomson, J. Barton. CREST Demand Model. Loughborough University. Dataset. (2015). Available online: https://doi.org/10.17028/rd.lboro.2001129.v8 (Accessed on 13 June 2024).
17. AliExpress, FLTXNY_FS_Model. Available online: https://it.aliexpress.com/item/1005005066900234.html?pdp_npi=2%40dis%21EUR%21488%2C33%E2%82%AC%21488%2C33%E2%82%AC%21%21%21%21%21%40211b813b16854350504741675e3fcd%2112000031506951497%21btf&_t=pvid%3Afc384f7b-933a-4d07-bcb1-3f831f498375&afTraceInfo=1005005066900234__pc__pcBridgePPC__xxxxxx__1685435050&spm=a2g0o.ppclist.product.mainProduct&gatewayAdapt=glo2ita (Accessed on 18 April 2024).
18. Strong Engineering and Consultant CO. LTD, DS-3000. Available online: https://www.sec.co.th/product/wind-turbine/ds3000 (Accessed on 18 April 2024).
19. ETNEO, DS-3000. Available online: https://etneo.com/prodotto/eolico-verticale-ibrido-3000w/ (Accessed on 18 April 2024).
20. AEOLOS Aeolos-V5. Available online: https://www.windturbinestar.com/mini-eolico-verticale-5kw.html (Accessed on 18 April 2024).
21. AEOLOS Aeolos-V5. Available online: https://store-7wpeis.mybigcommerce.com/aeolos-aeolos-v-5000w-5000w-off-grid-wind-turbine/ (Accessed on 18 April 2024).
22. AEOLOS Aeolos-V5. Available online: https://it.wind-turbine-models.com/turbines/1853-aeolos-aeolos-v-5kw (Accessed on 18 April 2024).
23. A. Rosato, A. Ciervo, G. Ciampi, M. Scorpio, F. Guarino, S. Sibilio. Energy, Environmental and economic dynamic assessment of a solar hybrid heating network operating with a seasonal thermal energy storage serving an Italian small-scale residential district: Influence of solar and back-up technologies, Therm. Sci. Eng. Prog. **19,** (2020).
24. S. Sibilio, G. Ciampi, A. Rosato, E. Entchev, W. Yaici. Parametric Analysis of a Solar Heating and Cooling System for an Italian Multi-Family House, Int. J. Heat Tech. **34**, (2016): 458-464.
25. G. Ciampi, S. Sibilio, A. Rosato. Yearly operation of a building-integrated microcogeneration system in south Italy: Energy and economic analyses, Int. J. Low Carbon Technol. **9**, (2014): 331-346.
26. G. Chicco, P. Mancarella. Assessment of the greenhouse gas emissions from cogeneration and trigeneration systems. Part I: Models and indicators, Energy **33**, (2008): 410-417.
27. S.A. Klein, TRNSYS 16: A Transient System Simulation Program - Volume 9 Weather Data, Solar Energy Laboratory, University of Wisconsin, Madison, USA, 2005. Available online: https://web.mit.edu/parmstr/Public/Documentation/09-WeatherData.pdf (Accessed on 18 April 2024).
28. Electricity Maps. https://www.electricitymaps.com/ (Accessed on 18 April 2024).
29. GME Gestore Mercati Energetici. Available online: https://www.mercatoelettrico.org/it/Statistiche/ME/PrezzoMedioFasce (Accessed on 18 April 2024).
30. ARERA Italian Regulatory Authority for Energy, Networks and Environment. Available online: https://www.arera.it/atti-e-provvedimenti (Accessed on 18 April 2024).